Conformation of Amylose in Dimethyl Sulfoxide

Yasushi Nakanishi, Takashi Norisuye,* and Akio Teramoto

Department of Macromolecular Science, Osaka Univeristy, Toyonaka, Osaka 560, Japan

Shinichi Kitamura

Department of Agricultural Chemistry, Kyoto Prefectural University, Shimogamo, Kyoto 606, Japan

Received March 1, 1993; Revised Manuscript Received May 3, 1993

ABSTRACT: The conformation of amylose in dimethyl sulfoxide (DMSO) at 25 °C is studied by light scattering, sedimentation equilibrium, and viscosity measurements on narrow-distribution samples of amylose and its oligomers covering a broad range of weight-average molecular weight M_w from 342 (the dimer) to 1.7 × 10^6. For M_w above 10^5, the z-average mean-square radius of gyration $\langle S^2 \rangle_z$ and the intrinsic viscosity $[\eta]$ vary as $M_w^{1.2}$ and $M_w^{0.7}$, respectively, indicating that in this molecular weight region, the amylose chain behaves as a random coil expanded by excluded-volume effect. Below $M_w \sim 10^4$, $[\eta]$ exhibits an unusually weak dependence on M_w and finally becomes almost independent of molecular weight. This behavior of $[\eta]$ is explained by solvation of DMSO molecules and some helical nature of the amylose chain on the basis of the theory of Yoshizaki et al. for unperturbed helical wormlike chains. The estimated stiffness parameter is comparable to that for atactic poly(methyl methacrylate), a flexible chain, being consistent with the above conclusion from the $\langle S^2 \rangle_z$ and $[\eta]$ data for M_w above 10^5. The characteristic ratio at infinite molecular weight is found to be about 5, a value close to the reported values for aqueous amylose. Thus it is further concluded that without excluded-volume effect, the conformations of high molecular weight amylose in water and DMSO are similar.

Introduction

Despite much experimental work done on dilute solutions of amylose, the conformation of the polysaccharide chain in dimethyl sulfoxide (DMSO) is still a matter of controversy. The reported intrinsic viscosity ($[\eta]$) versus weight-average molecular weight (M_w) relations are at variance, the viscosity exponent ν being 0.64 (Everett and Foster[1]), 0.70 (Banks and Greenwood[2]), 0.82 (Burchard[3]), 0.87 (Cowie[4]), and 0.91 (Fujii et al.[5]). The first two groups[1,2] proposed a random coil conformation for amylose in DMSO, while the last two groups[4,5] concluded the chain to be semirigid and predominantly helical. These conflicting molecular pictures coming primarily from ν indicate considerable difficulty in accurate determination of M_w.

Some of the above groups[4-6] also determined z-average mean-square radii of gyration $\langle S^2 \rangle_z$ for amylose samples in DMSO. Interestingly, all the $\langle S^2 \rangle_z$ data exhibited molecular weight dependences weaker than that for Gaussian chains. Such dependence seems plausible if the amylose chain is unperturbed by intramolecular excluded-volume effect and helical to some extent as is the case with atactic poly(methyl methacrylate) in Θ solvents.[7,8] However, the $[\eta]$–M_w relations mentioned above or their analyses[5,9] suggest that excluded-volume effects on $[\eta]$ are appreciable at least at high M_w, and thus the measured $\langle S^2 \rangle_z$ and $[\eta]$ by the previous groups are not always consistent.

This inconsistency and the above-mentioned discrepancy in ν motived us to examine the molecular weight dependence of $[\eta]$ and $\langle S^2 \rangle_z$ for amylose in DMSO and to deduce the global conformation of the polysaccharide chain. To this end we deemed it important to use synthetic amylose samples free from branching, since samples extracted from natural products often contain amylopectin. Thus we prepared narrow-distribution samples of synthetic amylose ranging in M_w from 5.6 × 10^3 to 1.7 × 10^6 and monodisperse maltodextrins of molecular weights from 342 to 2448 and investigated their DMSO solutions at 25 °C by light scattering, sedimentation equilibrium, and viscometry; $\langle S^2 \rangle_z$ was determined for samples with M_w higher than 1.8 × 10^5. The data for $\langle S^2 \rangle_z$ and $[\eta]$ obtained as functions of M_w are presented and analyzed below.

Experimental Section

Samples. Maltose (designated here as G-2), maltotriose (G-3), maltopentaose (G-5), maltohexaose (G-6), and maltoheptaose (G-7) were purchased from Hayashibara Biochemical Laboratories, Inc. (Okayama, Japan) and maltooctaose (G-8) and maltopentadecaose (G-15) from Nakano Vinegar Co. (Handa, Japan). The first sample G-2 had a purity of higher than 99.9% (manufacturer's data) and was used without further purification. The other maltodextrin samples were purified by gel-filtration chromatography on a Biogel P-2 column (Extra Fine, 1.5 × 120 cm or 2.5 × 100 cm) with water as the eluent. Their purity was checked by high-performance liquid chromatography with an NH_2-bonded silica column. A single peak was observed for each sample at the expected retention time. The molecular weights M of samples G-5, G-6, G-7, G-8, and G-15 were confirmed by fast atom bombardment mass spectrometry (JEOL-JMS-SX102A mass spectrometer). The accelerating voltage was 10 kV for G-5 to G-8 and 5 kV for G-15. Xenon was used as the bombarding gas, and the atom gun was operated at 6 kV.

Amylose samples were synthesized enzymatically from maltopentaose (the primer) and glucose 1-phosphate using potato phosphorylase. The procedures employed were essentially the same as those described elsewhere;[10] they are known to yield amylose narrow in molecular weight distribution. The phosphorylase purified from potato tubers according to the method of Kamogawa et al.[11] was free from any other carbohydrase activity. The molecular weights of the final products (amylose) were controlled by adjusting the concentration of the primer in the reaction mixture and the incubation period. After the incubation for the desired time period, each product was reprecipitated into ethanol, washed first with a water–ethanol (1:1 (v/v)) mixture once and then with ethanol and diethyl ether, each 3 times, and finally dried in vacuo. A high molecular weight synthetic sample, designated below as A-11, was supplied by Nakano Vinegar Co.

The amylose samples thus obtained were divided each into three to five parts by fractional precipitation with DMSO as the solvent and ethanol as the precipitant, but, in actuality, four of them including A-11 were used without fractionation because of the very limited quantities. Each fraction was reprecipitated

0024-9297/93/2226-4220$04.00/0

from a DMSO solution into ethanol, washed with ethanol, diethyl ether, and acetone, each three times, and dried in vacuo for 3 days. From the fractions thus prepared, appropriate middle ones were chosen for the present work, along with the four unfractionated samples similarly purified. These samples were designated as A-1, A-2, ..., and A-11 in order of increasing M (A-1, A-2, A-4, and A-11 are unfractionated).

Preparation of Test Solutions. Just before the preparation of DMSO solutions, a given sample was further dried in vacuo at 70–80 °C for 24 h. It was then dissolved in DMSO at room temperature. For samples A-1 through A-6, clear solutions were obtained by heating at 100 °C for 1 h in nitrogen-filled flasks. Heating at 100 °C within 3 h was found to cause no detectable degradation when checked with a higher molecular weight sample A-8 by viscometry. The polymer mass concentration c was calculated from the gravimetrically determined polymer weight fraction and the solution density. The DMSO used was fractionally distilled under a reduced nitrogen atmosphere after being dehydrated with calcium hydride.

Light Scattering. Intensity measurements were made at 25 °C for five high molecular weight samples A-7 through A-11 on a Fica 50 light scattering photometer in an angular range from 30 to 150°; for sample A-11, the measurement was made down to 22.5°. Use was made of vertically polarized incident light of 436- and 546-nm wavelengths. Pure benzene of 25 °C was used to calibrate the photometer. Its Rayleigh ratio was taken to be 46.5×10^{-6} cm^{-1} for 436 nm and 16.1×10^{-6} cm^{-1} for 546 nm[12] and its depolarization ratio was determined to be 0.41_0 for 436 nm and 0.39_6 for 546 nm by the method of Rubingh and Yu.[13] DMSO solutions of amylose and the solvent were optically clarified by filtration through Teflon Millipore filters with a pore size of 0.2 or 0.5 μm, followed by centrifugation at 2.5×10^4 gravities for 2 h (see also ref 14).

The intensity data obtained were analyzed by Berry's square-root plot[15] to evaluate M_w, $\langle S^2 \rangle_z$, and A_2 (the second virial coefficient) of each sample. Optical anisotropy effects on these quantities, though very small, were observed for samples A-7, A-8, and A-9 when measurements were made with an analyzer set in the horizontal direction. The correction made according to the conventional method[16] for flexible chains (see below for the conformation of amylose) was about 1% for M_w and $\langle S^2 \rangle_z$ and about 2% for A_2.

The specific refractive index increment $(\partial n/\partial c)$ of amylose in DMSO at 25 °C was determined, using a modified Schulz–Cantow type differential refractometer. The results at 436 and 546 nm were 0.060_7 and 0.061_5 cm^3 g^{-1}, respectively. The former is slightly smaller than the latter. This is unusual, but the reason is not clear to us. Burchard[17] observed the same trend for aqueous amylose.

Our $(\partial n/\partial c)$ values are much smaller than those (0.0676 and 0.0659 cm^3 g^{-1} at 436 and 546 nm, respectively) reported by Everett and Foster[6] and Fujii et al.[5] but rather close to Jordan and Brant's value[18] 0.062 cm^3 g^{-1} at 436 nm for dialyzed DMSO solutions containing 10 vol % water. Dintzis and Tobin[19] reported a value of about 0.06 cm^3 g^{-1} in DMSO at 546 nm, but they remarked that $(\partial n/\partial c)$ increased to about 0.07 cm^3 g^{-1}, a value close to that of Everett and Foster, when DMSO solutions were dialyzed. However, no such change in $(\partial n/\partial c)$ can be expected to occur for any two-component systems. In fact, we confirmed with our samples that $(\partial n/\partial c)$ stays unchanged before and after dialysis.

Ultracentrifugation. Values of M_w and A_2 for amylose samples A-1 through A-7 in DMSO at 25 °C were determined by sedimentation equilibrium in a Beckman Spinco Model E ultracentrifuge. A Kel-F 12-mm double sector cell was used. The solution column was adjusted to 1.2–1.5 mm and the rotor speed was chosen so that the equilibrium polymer concentration c_b at the cell bottom is about 3 times the concentration of c_a at the meniscus.

The data obtained were analyzed according to the equation[20]

$$M_{app}^{-1} = M_w^{-1} + 2A_2\bar{c} + \dots \quad (1)$$

where the apparent molecular weight M_{app} and the mean concentration $\bar{c}$ are defined by

$$M_{app} = (c_b - c_a)/\lambda c_0 \quad (2)$$

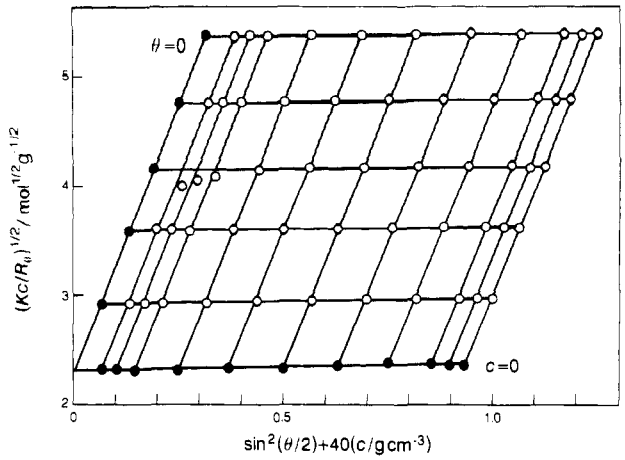

Figure 1. Zimm plot in the square-root form for amylose sample A-7 in DMSO at 25 °C and 546 nm.

$$\bar{c} = (c_a + c_b)/2 \quad (3)$$

with

$$\lambda = (r_b^2 - r_a^2)(1 - \bar{v}\rho_0)\omega^2/2RT \quad (4)$$

In these equations, r_a and r_b are the radial distances from the center of rotation to the meniscus and the cell bottom, respectively, $\bar{v}$ is the partial specific volume of the polymer, ρ_0 is the solvent density, ω is the angular velocity of the rotor, R is the gas constant, and T is the absolute temperature.

Ratios of M_z (the z-average molecular weight) to M_w were estimated from the sedimentation equilibrium data by use of the equation[21]

$$Q = (M_w/M_z)(1 + 2A_2M_w\bar{c} + \dots) \quad (5)$$

where

$$Q = \frac{(c_b - c_a)^2}{c_0(r_b^2 - r_a^2)[(\partial c/\partial r^2)_{r=r_b} - (\partial c/\partial r^2)_{r=r_a}]} \quad (6)$$

The partial specific volume of amylose in DMSO at 25 °C was determined to be 0.618 cm^3 g^{-1}, using a bicapillary pycnometer of about 30-cm^3 capacity. Additional density measurements on maltose gave essentially the same value, indicating that $\bar{v}$ of amylose in DMSO is quite insensitive to M.

Viscometry. Viscosities of DMSO solutions at 25 °C were measured for all samples using capillary viscometers of the Ubbelohde type having flow times of about 200 s for the solvent. In evaluation of relative viscosities for low molecular weight samples with $[\eta] < 100$ cm^3 g^{-1}, the difference between the solution and solvent densities was taken into account. The Huggins plot, the Fuoss–Mead plot, and the Billmeyer plot[22] were combined to determine $[\eta]$ and Huggins' constant k' for each sample.

Results

Molecular Weight, Second Virial Coefficient, and Radius of Gyration. Figures 1 and 2 illustrate the Zimm plots in the square-root form for samples A-7 and A-11, respectively, where K is the optical constant and R_θ, the reduced scattering intensity at scattering angle θ. These samples are the lowest and highest molecular weights studied in this work by light scattering. Their scattering envelopes are seen to be quite normal.

Figures 3 and 4 show, respectively, the plots of M_{app}^{-1} vs c and Q vs c constructed from sedimentation equilibrium data according to eqs 1 and 5. The straight lines in Figure 4 have been drawn with the aid of the A_2M_w values evaluated from the M_{app}^{-1} vs c plots in Figure 3. The values of M_w, A_2, and M_z/M_w obtained are summarized in Table I, along with those of M_w, A_2, and $\langle S^2 \rangle_z$ from light scattering. The following remarks are pertinent here.

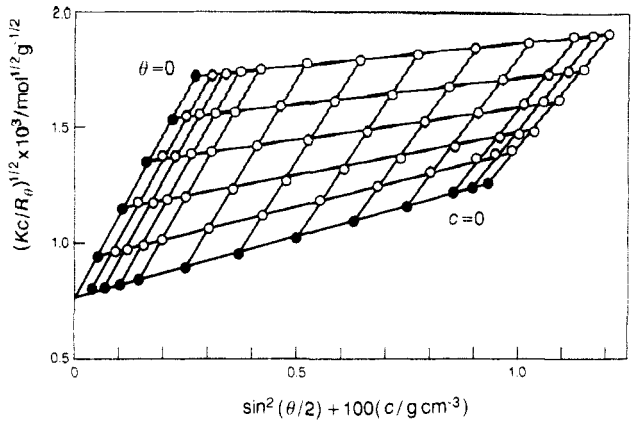

Figure 2. Zimm plot in the square-root form for amylose sample A-11 in DMSO at 25 °C and 546 nm.

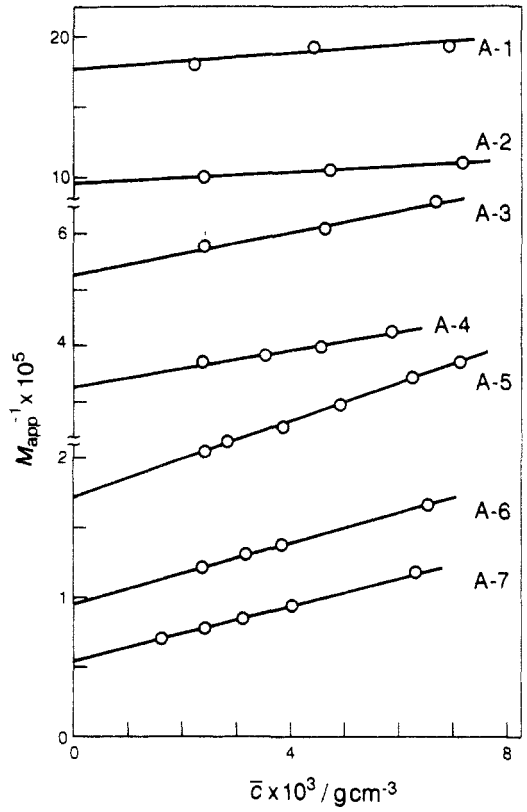

Figure 3. Plots of M_{app}^{-1} vs $\bar{c}$ for indicated amylose samples in DMSO at 25 °C.

(1) The M_z/M_w values indicate that samples A-1 through A-7 are sharp in molecular weight distribution. (2) The M_w value for sample A-7 from light scattering at 546 nm is in excellent agreement with that from sedimentation equilibrium. (3) However, the light scattering M_w for the same sample at 436 nm is larger by about 3% than these. Though small, similar discrepancies in light scattering M_w between 436 and 546 nm can be seen for the other fractions. This trend may have something to do with $(\partial n/\partial c)$ whose value at 436 nm was smaller by about 1.5% than that at 546 nm (see the Experimental Section). In the data analysis made below, we use the values at 546 nm for M_w and A_2. On the other hand, the mean of the $\langle S^2\rangle_z$ values at the two wavelengths is used for samples A-9, A-10, and A-11 since $\langle S^2\rangle_z$ is determined regardless of $(\partial n/\partial c)$.

The A_2 data are plotted double-logarithmically against M_w in Figure 5. They are represented approximately by a straight line with a slope of 0.29, but those for M_w above 5×10^4 are fitted by a line with slope 0.25 (not shown here). The latter slope is comparable to what is usually observed for flexible polymers in good solvents.

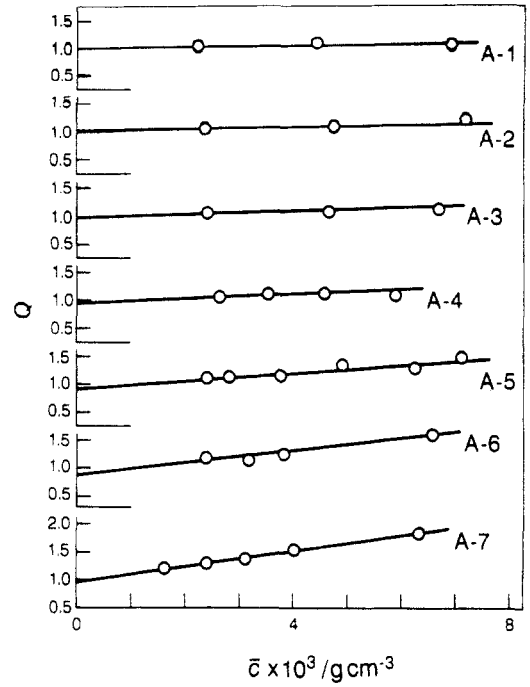

Figure 4. Plots of Q vs $\bar{c}$ for indicated amylose samples in DMSO at 25 °C. Q is defined by eq 6.

Table I. Results from Sedimentation Equilibrium and Light Scattering Measurements on Amylose Samples in DMSO at 25 °C

sample	$10^{-4}M_w$	M_z/M_w	10^4A_2, cm^3 mol g^{-2}	$\langle S^2\rangle_z$, nm^2
		Sedimentation Equilibrium		
A-1	0.562	1.0	14	
A-2	1.03	1.0	9.1	
A-3	1.89	1.0_5	9.13	
A-4	3.07	1.1	8.43	
A-5	5.82	1.1	6.76	
A-6	10.6	1.2	5.63	
A-7	18.5	1.0_5	4.94	
		Light Scattering		
A-7	18.6[a]		4.48[a]	
	19.1[b]		4.45[b]	260[b]
A-8	33.6[a]		4.07[a]	
	34.4[b]		4.01[b]	510[b]
A-9	46.4[a]		3.85[a]	690[a]
	47.7[b]		3.82[b]	680[b]
A-10	67.9[a]		3.81[a]	1310[a]
	69.4[b]		3.75[b]	1340[b]
A-11	172[a]		2.71[a]	3550[a]
	177[b]		2.70[b]	3590[b]

[a] At 546 nm. [b] At 436 nm.

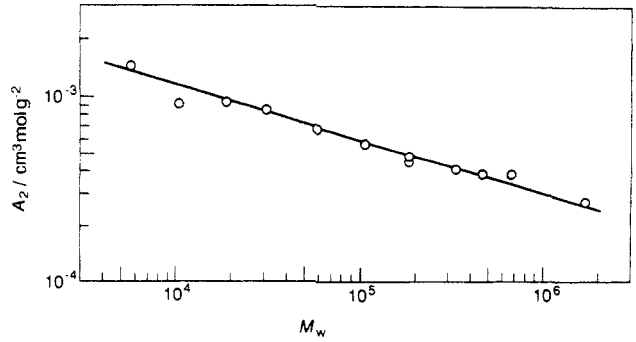

Figure 5. Molecular weight dependence of A_2 for amylose sample in DMSO at 25 °C.

The circles in Figure 6 show the present $\langle S^2\rangle_z$ data plotted double-logarithmically against M_w. The straight line fitting them has a slope 1.2, which is the exponent expected for long flexible chains in good solvents.[23] The other symbols in the figure represent the $\langle S^2\rangle_z$ data by the

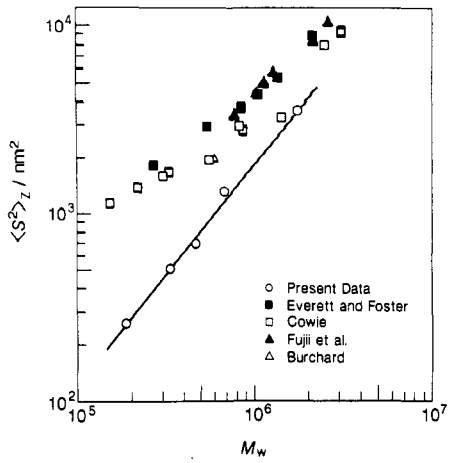

Figure 6. Molecular weight dependence of $\langle S^2\rangle_z$ for amylose in DMSO, determined by the indicated groups.[3-6]

Table II. Results from Viscosity Measurements on Amylose and Oligomer Samples in DMSO at 25 °C

sample	M	$[\eta]$, cm^3 g^{-1}	k'	sample	$10^{-4}M_w$	$[\eta]$, cm^3 g^{-1}	k'
G-2	342	6.04	0.64[a]	A-1	0.562	8.90	0.61[a]
G-3	504	6.06	0.85[a]	A-2	1.03	13.0	0.50[a]
G-5	828	6.45	0.66[a]	A-3	1.89	17.4	0.52
G-6	990	6.36	0.53[a]	A-4	3.07	25.0	0.35
G-7	1152	6.47	0.51[a]	A-5	5.82	36.3	0.41
G-8	1314	6.47	0.61[a]	A-6	10.6	57.5	0.36
G-15	2448	6.95	0.72[a]	A-7	18.6	85.2	0.36
				A-8	33.6	129	0.35
				A-9	46.4	157	0.34
				A-10	67.9	200	0.39
				A-11	172	410	0.40

[a] Estimated on the assumption that the partial specific volume is independent of c.

indicated groups.[3-6] Strikingly, all these data come far above ours, the discrepancy being more remarkable at lower M_w. The much larger $\langle S^2\rangle_z$ values by the previous workers may be attributed partly to the samples' polydispersity. Everett and Foster[6] and Cowie[4] inferred that their samples had an M_z/M_w of about 1.3, while Fujii et al.[5] argued that for their $\langle S^2\rangle_z$ data to be consistent with sedimentation coefficient data, M_z/M_w had to be about 1.6. Besides such polydispersity effects,[24] qualitative differences between the light scattering envelopes of these authors and ours cannot be overlooked. Fujii et al. observed pronounced downward curvatures at low scattering angles for a sample ($M_w = 7.8 \times 10^5$) even in the linear plot of Kc/R_θ vs $\sin^2(\theta/2)$. Such curvatures are most likely due to the presence of microgels or aggregates in the DMSO solutions. The Zimm plots reported by Everett and Foster and Cowie exhibit angular dependences of Kc/R_θ stronger at higher c, also suggesting the presence of such large particles, at least, in solutions of high c.

Intrinsic Viscosity. Table II summarizes the values of $[\eta]$ and k' for all amylose and oligomer samples together with the molecular weights; the M_w values for the A-series samples are the reproductions from Table I. The molecular weight dependence of $[\eta]$ is displayed in Figure 7, in comparison with the published data[1-5] including those of Banks and Greenwood,[2] who estimated the molecular weights for amylose samples from the measured M_w for amylose triacetate samples. Our data points (the circles) come close to those of this group and of Burchard;[3] the last author determined M_w by light scattering with water as the solvent. The data of Fujii et al.[5] for the three highest molecular weight fractions are consistent with ours, but as M_w decreases, the discrepancy becomes large.

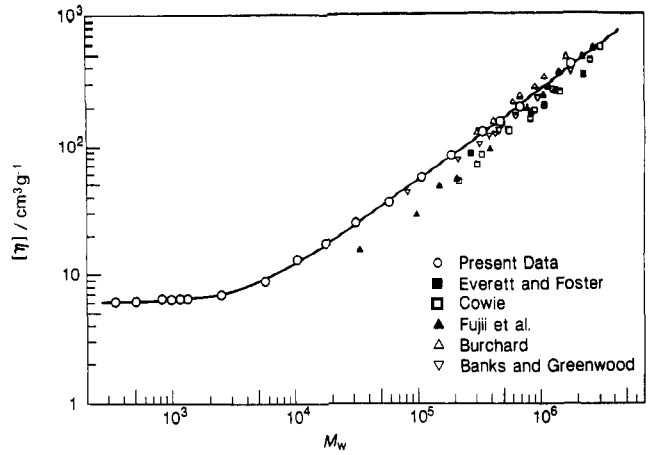

Figure 7. Molecular weight dependence of $[\eta]$ for amylose in DMSO, determined by the indicated groups.[1-5]

The present $[\eta]$ data for M_w above 5×10^4 in Figure 7 are fitted by a straight line with slope 0.7. This ν value is typical of long flexible chains in good solvents and thus seems consistent with our $\langle S^2\rangle_z$ data in Figure 6. As the molecular weight is lowered, ν decreases and becomes almost zero for M_w below 10^3. This unusually small ν in the oligomer region was found early by Burchard,[3] who determined the molecular weights of oligomer samples by the ferricyanide method.

The $[\eta]$ value of about 6 cm^3 g^{-1} for maltose (see Table II) is much larger than the value 1.55 cm^3 g^{-1} calculated from the Einstein equation for rigid spheres with the specific volume equated to $\bar{v}$. When $[\eta]$ of maltose was measured in water at 25 °C, a value of 2.61 cm^3 g^{-1}, less than half that in DMSO, was obtained. Further, $[\eta]$ for pentamaltose in water at 25 °C was found to be 3.51 cm^3 g^{-1}, which is also much smaller than the corresponding value 6.45 cm^3 g^{-1} in DMSO. These findings strongly suggest that DMSO molecules solvate glucose residues, thereby increasing the hydrodynamic volume of the oligomer or polysaccharide chain. The presence of such solvation onto amylose and model compounds is already evidenced by ^{1}H NMR measurements.[25,26] It should be noted that the possibility of aggregate formation of maltodextrins in DMSO is ruled out since addition of acetone, a nonsolvent for amylose, lowers $[\eta]$.[3]

Discussion

Random Coil of High Molecular Weight Amylose. The molecular weight dependence of $\langle S^2\rangle_z$ and $[\eta]$ determined in this work gives no evidence for semirigidity of the amylose chain in DMSO but is consistent with the view that the chain is flexible. Except for sample A-9, the data of M_w, A_2, $\langle S^2\rangle_z$, and $[\eta]$ in Tables I and II yield 0.27–0.30 for the interpenetration function [$\equiv A_2M^2/(4\pi^{3/2}N_A\langle S^2\rangle^{3/2})$, with N_A the Avogadro constant] and (1.9–2.6) $\times 10^{23}$ mol^{-1} for the Flory viscosity factor [$\equiv[\eta]M/(6\langle S^2\rangle^{3/2})$]. Moreover, the dimensionless quantity $A_2M/[\eta]$ is found to be 1.04–1.27 for $M_w > 5 \times 10^4$ from the same data. All these values are predictable for flexible chains in good solvents.[16,23] Thus, the present data for M_w, A_2, $\langle S^2\rangle_z$, and $[\eta]$ demonstrate in a consistent way that the overall chain conformation of amylose with $M_w > 10^5$ in DMSO is a random coil expanded by excluded-volume effect.

Viscosity Behavior of Low Molecular Weight Amylose. A remarkable feature of amylose in DMSO is that its $[\eta]$ is almost independent of molecular weight in the range from 342 (maltose) to 1.31×10^3 (maltooctaose) and then gradually increases for $M_w < 10^4$. In the following,

we attempt to explain this unusually weak M dependence of $[\eta]$ on the basis of the theory of Yoshizaki, Nitta, and Yamakawa[27] for $[\eta]$ of a touched-bead helical wormlike (HW) chain, with solvation of DMSO molecules taken explicitly into account. No excluded-volume effect is considered, since our data analysis is concerned with low M.

The theory of Yoshizaki et al. contains five parameters, the contour length L of the chain (or the number N of beads in the chain), the stiffness parameter λ^{-1}, the differential geometrical curvature κ_0 and torsion τ_0 of the characteristic regular helix taken at the minimum energy of the HW chain,[28] and the diameter d of each bead. The first parameter, equal to Nd, is related to M by

$$L = M/M_L \tag{7}$$

with M_L being the molar mass per unit contour length of the chain. When $L = d$ (i.e., $N = 1$), the expression of Yoshizaki et al. gives the Einstein equation for rigid spheres. The HW chain with zero κ_0 is identical to the Kratky–Porod (KP) wormlike chain,[29] regardless of τ_0, as far as properties such as $[\eta]$ and $\langle S^2 \rangle$ dependent only on the chain contour are concerned.[28] In this special case, $1/(2\lambda)$ is equal to the persistence length. It should be noted that the contour of the KP chain with the minimum energy is a straight rod and thus has no helical nature.

Assuming that solvation of DMSO molecules takes place over the entire amylose chain surface including both chain ends, we may write the effective diameter d' and effective contour lenght L' of solvated amylose (hydrodynamically equivalent to the touched-bead model chain) as

$$d' = d + \Delta \tag{8}$$

$$L' = L + \delta = (M/M_L) + \delta \tag{9}$$

Here, Δ and δ denote, respectively, the increases of diameter and contour length due to the solvation.

We have six unknown parameters, M_L, d', δ, λ^{-1}, κ_0, and τ_0. Arbitrariness in finding their unique set is considerably diminished by the availability of $[\eta]$ data at very low M where the theoretical $[\eta]$ is determined substantially by the first three parameters, i.e., M_L, d', and δ. Thus, with appropriate parameter sets assumed for λ^{-1}, κ_0, and τ_0, we first searched for a set of M_L, d', and δ allowing the theory of Yoshizaki et al. to explain the nearly constant values of $[\eta]$ for M between 342 and 1.31×10^3, but found that the length of one bead, d', cannot be smaller than L' of the solvated dimer ($M = 342$). This forced us to view the amylose chain on a large length scale, and we decided to take the solvated dimer to be one bead as the smallest length scale possible in our analysis. Under this condition, M_L, d', and δ were uniquely determined to be 500 nm^{-1}, 1.4 nm, and 0.70 nm, respectively. These values were then used to estimate the remaining parameters (λ^{-1}, κ_0, and τ_0) by curve-fitting in a molecular weight range as wide as possible. Equally close fits were found over the range of M from 342 to 1×10^4 for several parameter sets within the ranges of λ^{-1}, κ_0/λ, and τ_0/λ from 3.5 to 4.5 nm, from 3 to 4, and from 3 to 5, respectively.

An example is shown in Figure 8, in which for clarity, the theoretical $[\eta]$ values computed for $\lambda^{-1} = 4.0$ nm, $\kappa_0/\lambda = 3.5$, and $\tau_0/\lambda = 4.0$ with $M_L = 500$ nm^{-1}, $d' = 1.4$ nm, and $\delta = 0.70$ nm are connected by a solid line for $N > 2$ and by a dashed line for N between 1 and 2; the arrows point the molecular weights corresponding to $N = 1$ and 2. The systematic downward deviation of the solid curve from the data points for $M_w > 10^4$ may be ascribed to excluded-volume effects.

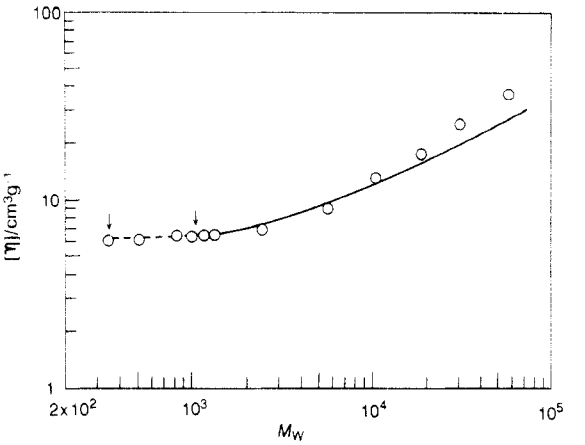

Figure 8. Comparison between experimental and theoretical $[\eta]$: circles, present data for amylose in DMSO; curve, calculated from the theory of Yoshizaki et al.[27] for unperturbed helical wormlike chains with $M_L = 500$ nm^{-1}, $d' = 1.4$ nm, $\delta = 0.7$ nm, $\lambda^{-1} = 4.0$ nm, $\kappa_0/\lambda = 3.5$, and $\tau_0/\lambda = 4.0$ (see text for the significance of the arrows).

When amylose was modeled by the KP wormlike chain, the "closest" fit was found for $\lambda^{-1} = 2.4$ nm (i.e., 1.2 nm for the persistence length) with the same parameter values for M_L, d', and δ as estimated above, but it was somewhat worse than that exemplified in Figure 8. Importantly, this λ^{-1} value, which is comparable to 2.3 nm for atactic polystyrene (a-PS),[30,31] a typical flexible chain, is unreasonably small. Thus, the KP chain is not a relevant model for amylose in DMSO.

As can be seen from eq 9, the contribution of δ to L' diminishes with increasing M. Our analysis shows that this gives a decrease in hydrodynamic volume (per 1 g of amylose) and offsets a normal increase in $[\eta]$ with increasing L, leading to M-independent $[\eta]$ for $M < 1.3 \times 10^3$. We note that because of the presence of the solvent layers at the chain ends, the average number of glucose residues contained in one bead increases to about 4 at high M where δ is negligible compared to L. In the region of M_w between 2×10^3 and 10^4, the molecular weight dependence of $[\eta]$ is still weak. It may be due partly to the solvation effect but predominantly to some helical nature of the amylose chain as indicated by nonzero κ_0.

When M_w exceeds 10^4, excluded-volume effects become appreciable. This critical molecular weight for the onset of volume effect corresponds to a reduced contour length λL of about 5, which may be compared favorably with those (3–6) reported for a-PS[30] and atactic poly(methyl methacrylate) (a-PMMA),[8] both flexible chains, in good solvents.

HW Model Parameters and Conformational Characteristics. The M_L value of 500 nm^{-1} estimated above is appreciably larger than the value 380 nm^{-1} obtained from M_0 (the molar mass of glucose residue) = 162 and l (the virtual bond length of a glucose unit) = 0.425 nm.[32] This difference seems reasonable since our data analysis is concerned with a large length scale of two to four glucose units. It should be noted that if amylose in DMSO locally maintained the 6_1 helical structure with pitch 0.8 nm,[33] M_L would be as large as 1200 nm^{-1}. The solvent layer thickness $\delta/2$ of 0.35 nm is slightly smaller than the monolayer value 0.5 nm which can be estimated from the size of one DMSO molecule. The bead diameter for unsolvated amylose is calculated to be about 0.7 nm from eq 8 with $d' = 1.4$ nm and $\Delta \approx \delta = 0.7$ nm. This d value is also reasonable as compared to the chemical structure of the polysaccharide. More importantly, the stiffness parameter λ^{-1} of 4 (± 0.5) nm is at least 1 order of magnitude

smaller than those for typical semiflexible polymers.[23,28] It is comparable to 4.5–5.8 nm for a-PMMA[7,8] known as a flexible chain having unmistakable helical nature.

Though flexible, the amylose chain should also have a certain helical conformation locally, as indicated by the estimated HW parameters. This is consistent with what has been predicted by conformational analysis.[34] The pitch h [$=2\pi\tau_0/(\kappa_0^2 + \tau_0^2)$] of the amylose characteristic helix (at the minimum energy)[28] is calculated to be about 3.5 nm, if use is made of $\lambda^{-1} = 4.0$ nm, $\kappa_0/\lambda = 3.5$, and $\tau_0/\lambda = 4.0$. This h value is about twice that (1.7 nm) estimated on a certain large length scale by Yamakawa and coworkers,[35] who applied the HW model to Jordan et al.'s conformation calculations[34] on the persistence vector and mean-square end-to-end distance of amylose in water. However, not much significance may be put on this discrepancy, because the value of h depends on the length scale adopted in analysis.[28,35]

The characteristic ratio C_∞ is independent of length scale and pertinent to discussions on the global conformation of amylose with which the present work is primarily concerned. It is expressed by

$$C_\infty = (6M_0/l^2)(\langle S^2\rangle_0/M)_\infty \quad (10)$$

with $\langle S^2\rangle_0$ being the unperturbed mean-square radius gyration; the subscript ∞ signifies the limit of infinite M. For an HW chain, $(\langle S^2\rangle_0/M)_\infty$ is given by[36]

$$(\langle S^2\rangle_0/M)_\infty = (4\lambda^2 + \tau_0^2)/[6\lambda M_L(4\lambda^2 + \kappa_0^2 + \tau_0^2)] \quad (11)$$

Substituting $M_L = 500$ nm^{-1}, $\lambda^{-1} = 4.0$ nm, $\kappa_0/\lambda = 3.5$, and $\tau_0/\lambda = 4.0$, we obtain 8.3×10^{-4} nm^2 for $(\langle S^2\rangle_0/M)_\infty$, which in turn yields $C_\infty = 4.5$ if the l value of 0.425 nm is again used. As anticipated, substantially the same C_∞ values are obtained from most of the other parameter sets that led to close fits indistinguishable from what is shown in Figure 8 (exceptionally small C_∞ values of 4.2 and 4.3 are obtained only for two parameter sets, i.e., for $\lambda^{-1} = 4.0$ nm and $\kappa_0/\lambda = \tau_0/\lambda = 3.0$ and for $\lambda^{-1} = 3.5$ nm, $\kappa_0/\lambda = 3.0$, and $\tau_0/\lambda = 4.0$). Thus, some arbitrariness in our HW parameter values gives no large uncertainty in C_∞.

A larger error may come from the theory of Yoshizaki et al.[27] (or any current polymer hydrodynamic theory[16,23]), which overestimates $[\eta]$ or the Flory viscosity factor for unperturbed long flexible chains (Gaussian chains) by 3–23% depending on polymer + Θ solvent system.[37] In other words, $(\langle S^2\rangle_0/M)_\infty$ and hence C_∞ evaluated on the basis of the current $[\eta]$ theory should be underestimated by 2–15%. Thus, it seems reasonable to conclude that C_∞ of amylose in DMSO at 25 °C is 5 ± 0.8.

This value is close to those (5 ± 1) reported for aqueous amylose by many workers.[38,39] The agreement indicates that without excluded volume effect, the global conformations of the polysaccharide chain in water and DMSO are essentially the same and hence that solvation of DMSO molecules hardly stiffens the chain. These are consistent with Jordan and Brant's finding that C_∞ values in water–DMSO mixtures are insensitive to DMSO composition.

Conclusions

The major conclusions drawn in this work may be summarized as follows.

1. The intrinsic viscosity of amylose in DMSO at 25 °C exhibits an unusually weak M dependence for M_w below 10^4. This behavior of $[\eta]$ can be explained almost quantitatively by the theory of Yoshizaki et al.[27] for unperturbed helical wormlike chains when solvation of DMSO molecules onto the polysaccharide chain is taken into account.

2. The amylose chain in DMSO has some helical nature but is as flexible as atactic poly(methyl methacrylate). Its C_∞ (about 5) does not differ from that in water, and hence without volume effect, the global conformations in the two solvents are essentially the same.

3. Intramolecular excluded-volume effects on $[\eta]$ in DMSO become appreciable when M_w exceeds 10^4. Above $M_w \sim 10^5$, the amylose chain assumes a random coil conformation, as early concluded by Everett and Foster[1] and by Banks and Greenwood.[2]

Acknowledgment. This work was supported by a Grant-in-Aid (04453107) for Scientific Research from the Ministry of Education, Science and Culture, Japan.

References and Notes

(1) Everett, W. W.; Foster, J. F. *J. Am. Chem. Soc.* **1959**, *81*, 3464.
(2) Banks, W.; Greenwood, C. T. *Carbohydr. Res.* **1968**, *7*, 414.
(3) Burchard, W. *Makromol. Chem.* **1963**, *64*, 110.
(4) Cowie, J. M. G. *Makromol. Chem.* **1961**, *42*, 230.
(5) Fujii, M.; Honda, K.; Fujita, H. *Biopolymers* **1973**, *12*, 1177.
(6) Everett, W. W.; Foster, J. F. *J. Am. Chem. Soc.* **1959**, *81*, 3459.
(7) Tamai, Y.; Konishi, T.; Einaga, Y.; Fujii, M.; Yamakawa, H. *Macromolecules* **1990**, *23*, 4067.
(8) Fujii, Y.; Tamai, Y.; Konishi, T.; Yamakawa, H. *Macromolecules* **1991**, *24*, 1608.
(9) Banks, W.; Greenwood, C. T. In *Conformation of Biopolymers*; Remachandran, G. N., Ed.; Academic Press: New York, 1967; p 739.
(10) Kitamura, S.; Yunokawa, H.; Mitsuie. S.; Kuge, T. *Polym. J.* **1982**, *14*, 93.
(11) Kamogawa, S.; Fukui, T.; Nikuni, Z. *J. Biochem.* **1968**, *63*, 361.
(12) Deželić, Gj.; Vavra, J. *Croat. Chem. Acta* **1966**, *68*, 1106.
(13) Rubingh, D. N.; Yu, H. *Macromolecules* **1976**, *9*, 681.
(14) Kashiwagi, Y.; Norisuye, T.; Fujita, H. *Macromolecules* **1981**, *14*, 1220.
(15) Berry, G. C. *J. Chem. Phys.* **1966**, *44*, 4550.
(16) Yamakawa, H. *Modern Theory of Polymer Solutions*; Harper & Row: New York, 1971.
(17) Burchard, W. *Makromol. Chem.* **1963**, *59*, 16.
(18) Jordan, R. C.; Brant, D. A. *Macromolecules* **1980**, *13*, 491.
(19) Dintzis, F. R.; Tobin, R. *Carbohydr. Res.* **1978**, *66*, 71.
(20) Fujita, H. *Foundations of Ultracentrifugal Analysis*; Wiley: New York, 1975.
(21) Norisuye, T.; Yanaki, T.; Fujita, H. *J. Polym. Sci., Polym. Phys. Ed.* **1980**, *18*, 547.
(22) Billmeyer, F. W., Jr. *J. Polym. Sci.* **1949**, *4*, 83.
(23) Fujita, H. *Polymer Solutions*; Elsevier: Amsterdam, 1990.
(24) Burchard used a synthetic amylose sample. His large $\langle S^2\rangle_z$ value is most likely due to the use of the linear plot of Kc/R_θ vs $\sin^2(\theta/2)$, which overestimates $\langle S^2\rangle_z$ for narrow distribution samples.
(25) Casu, B; Reggiani, M.; Gallo, G. G.; Vigevani, A. *Tetrahedron Lett.* **1965**, 2253.
(26) Casu, B; Reggiani, M.; Gallo, G. G.; Vigevani, A. *Tetrahedron Lett.* **1966**, 22, 3061.
(27) Yoshizaki, T.; Nitta, I.; Yamakawa, H. *Macromolecules* **1988**, *21*, 165.
(28) Yamakawa, H. *Annu. Rev. Phys. Chem.* **1984**, *35*, 23.
(29) Kratky, O.; Porod, G. *Recl. Trav. Chim. Pays-Bas* **1949**, *68*, 1106.
(30) Einaga, Y.; Koyama, H.; Konishi, T.; Yamakawa, H. *Macromolecules* **1989**, *22*, 3419.
(31) Konishi, T.; Yoshizaki, T.; Saito, T.; Einaga, Y.; Yamakawa, H. *Macromolecules* **1990**, *23*, 290.
(32) Goebel, C. V.; Dimpfl, W. L.; Brant, D. A. *Macromolecules* **1970**, *3*, 644.
(33) Rundle, R. E.; French, D. *J. Am. Chem. Soc.* **1943**, *65*, 558.
(34) Jordan, R. C.; Brant, D. A.; Cesaro, A. *Biopolymers* **1978**, *17*, 2617.
(35) Fujii, M.; Nagasaka, K.; Shimada, J.; Yamakawa, H. *Macromolecules* **1983**, *16*, 1613.
(36) Yamakawa, H.; Fujii, M. *J. Chem. Phys.* **1976**, *64*, 5222.
(37) Konishi, T.; Yoshizaki, T.; Yamakawa, H. *Macromolecules* **1991**, *24*, 5614.
(38) Banks, W.; Greenwood, C. T. *Starch and its Components*; Edinburgh University Press: Edinburgh, 1975.
(39) Ring, S. G.; I'Anson, K. J.; Morris, V. J. *Macromolecules* **1985**, *18*, 182.